Chemical Engineering Science 203 (2019) 380–390

Contents lists available at ScienceDirect

Chemical Engineering Science

journal homepage: www.elsevier.com/locate/ces

Understanding mild cell disintegration of microalgae in bead mills for the release of biomolecules

E. Suarez Garcia [a,*], C. Lo [a], M.H.M. Eppink [a], R.H. Wijffels [a,b], C. van den Berg [a]

[a] Bioprocess Engineering, Wageningen University and Research, PO Box 16, 6700 AA Wageningen, the Netherlands
[b] Nord University, Faculty of Biosciences and Aquaculture, N-8049 Bodø, Norway

HIGHLIGHTS

- A model was developed to predict the rates of cell disintegration of microalgae.
- Cell disintegration (k_{dis}) can be quantified from cell-specific parameters.
- Energy efficiency is implemented from cell and equipment characteristics.
- The predicted k_{dis} can be used to estimate the selective release of biomolecules.
- The model has potential for bead mill optimization and scale up studies.

GRAPHICAL ABSTRACT

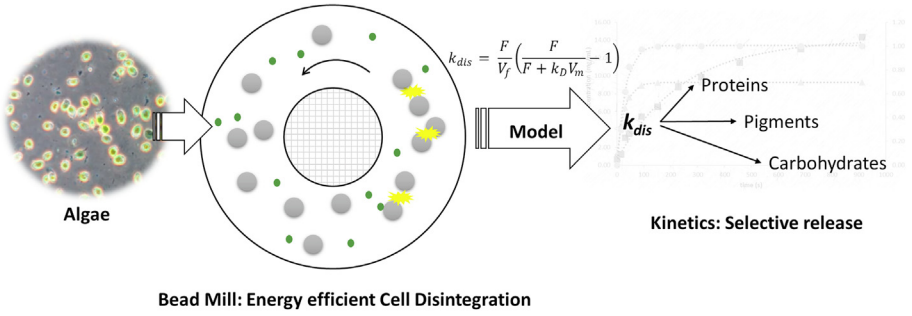

ARTICLE INFO

Article history:
Received 10 October 2018
Received in revised form 1 April 2019
Accepted 4 April 2019
Available online 5 April 2019

Keywords:
Bead mill
Energy efficient
Disintegration
Selective release
Microalgae
Biorefinery

ABSTRACT

Cell disintegration is, in general, the first step in the biorefinery of algae, since it allows the release of biomolecules of interest from the cells into the bulk medium. For high-value commercial applications, the disintegration process must be selective, energy efficient and mild. Developing a process with such features would demand extensive experimental effort. In the present study, we attempt to provide a tool for developing an efficient disintegration process via bead milling, by proposing a modelling strategy that allows the prediction of the kinetics of cell disintegration while having as input not only process parameters but also strain-specific parameters like cell size and cell-wall strength. The model was validated for two different algal strains (*Tetraselmis suecica* and *Chlorella vulgaris*), at various values of bead size (0.3–1 mm) and bead fillings (2.5–75%) and at two different scales of 80 and 500 mL. Since the kinetics of disintegration is proportional to the kinetics of release of biomolecules, the model can be further used for scale-up studies and to establish a window of operation to selectively target cells or metabolites of interest. Furthermore, the energy consumption in the mill was evaluated and it was found that operating at high bead fillings (>65%) is crucial to ensure an energy efficient process.

1. Introduction

Microalgae have gained attention in the last years as a sustainable feedstock, since their cultivation is not dependent on fresh water or arable land and can contribute to the mitigation of carbon emissions (Draaisma et al., 2013). Algae can accumulate a variety of biomolecules, which can serve multiple industries: proteins for food/feed applications (Vanthoor-Koopmans et al., 2013), carbohydrates for materials and biofuels (Chen et al., 2013), lipids for nutraceuticals and biofuels (Adarme-vega et al., 2012), pigments and specialty chemicals (Cuellar-Bermudez et al., 2015) for high

* Corresponding author.
E-mail address: edgar.suarezgarcia@wur.nl (E. Suarez Garcia).

https://doi.org/10.1016/j.ces.2019.04.008
0009-2509/

Nomenclature

Symbols

A	cross-sectional area of the gap between the accelerator and chamber wall [m]
C_X	algal biomass concentration in the suspension [g/kg]
d_b	bead diameter [m]
d_X	cell diameter [m]
E	total energy released by collisions [J s^{-1}]
E_b	energy released in a single impact event [J]
E_b	specific energy consumption [kWh $kgDW^{-1}$]
E_X	specific energy required to disrupt a single cell [J/cell]
F	recirculation flowrate [m^3/s]
k_{dis}	disintegration kinetic constant [s^{-1}]
L	effective length of the milling chamber [m]
n	number density of beads [bead/m^3]
n_X	number density of cells [cell/m^3]
n_{Xf}	number density of cells in the feeding compartment [cell/m^3]
$n_{X,out}$	number density of cells in the recirculation flow [cell/m^3]
u_b	bead velocity [m/s]
u_L	liquid velocity [m/s]
u_θ	azimuthal component of liquid velocity [m/s]
P	volumetric energy supply due to collisions [J m^{-3} s^{-1}]
R	the radius of the milling chamber [m]
r	radial position inside the milling chamber [m]
r_b	bead radius [m]
r_j	radial position of the centre of mass of bead at layer j [m]
t	Time [s]
V_b	volume of a single bead [m^3]
V_{ch}	volume of milling chamber [m^3]
V_f	remaining volume of suspension inside the feeding chamber [m^3]
V_{susp}	total volume of suspension [m^3]
V_X	volume of a single cell [m^3]
T	throughput of a bead mill [m^3/h]
z	collision frequency of beads per unit volume [m^{-3} s^{-1}]

Greek symbols

α	bead filling percentage
$\dot{\gamma}$	shear rate [s^{-1}]
ε	bead porosity due to packing
η	effective disintegration efficiency constant
κ	the ratio between the accelerator radius and the mill radius
μ	liquid dynamic viscosity [kg s^{-1} m^{-1}]
ρ_b	bead density [kg/m^3]
ρ_L	liquid density [kg/m^3]
Ω	angular velocity of the accelerator [s^{-1}]

end markets, just to name the most common applications. However, in order to recover the valuable biomolecules from algae, it is necessary to access the cell wall and/or membrane under mild conditions. To achieve this, several methods have been reported in literature, including physical, biological and chemical treatments (Dixon and Wilken, 2018; Günerken et al., 2015; Phong et al., 2018). Among these, bead milling has been proposed as an energy efficient, mild technology leading to complete cell disintegration and selective release in a short time (Suarez Garcia et al., 2018).

Bead mills have been extensively studied for applications in mineral processing and biotechnology (Kwade et al., 1996; Kula and Schütte 1987). However, investigations regarding microalgae biorefinery have been limited to disintegration studies (Postma et al., 2015) using statistical tools, residence time distribution analysis and kinetic studies (Montalescot et al., 2015) and application of the stress model (Montalescot et al., 2015; Postma et al., 2017; Zinkoné et al., 2018). The stress model developed by Blecher et al. (1996) and Kwade et al. (1996) for the comminution of minerals, is based on the existence of stress events that lead to shear and eventual disintegration. Both the intensity and the frequency of such events are taken into account to quantify the power transferred to the product and the corresponding comminution (crystalline materials) or disintegration extent (agglomerates and cells). However, in the case of cells, the model does not include cell properties and assumes that the beads move at a speed proportional to the tip speed. This is an important disadvantage as the beads develop a velocity profile in the milling chamber (Yamamoto et al., 2012).

A more complete theoretical understanding of the disintegration of microalgal cells in bead mills is lacking. It is important to take into consideration the mechanical properties of the cells, in particular cell-wall strength, which is dependent on the cell composition and size, as already known for yeast (Smith et al., 2000). Also equipment characteristics and process variables (e.g., bead size, bead filling ratio, agitation speed, flow rate) need to be taken into account. Furthermore, as the release of biomolecules - proteins, carbohydrates and pigments- is linked to the kinetics of cell disintegration (Postma et al., 2017; Suarez Garcia et al., 2018), a more clear understanding of the cell disintegration process can contribute to their design, operation, optimization and scale-up.

The present study aims at developing a modelling strategy for the disintegration of microalgae cells in bead mills. The model takes into consideration the mechanical properties of the cell as well as several process and equipment variables. We have included the concept of effective disintegration energy and have considered variable energy release as function of the mill radius. The model is validated with experimental data at various bead sizes and bead fillings, at two different scales and for two microalgae strains. We also propose that the kinetic constants can be used as a key parameter in process design studies, performance indicator, optimization and for scale-up purposes.

2. Material and methods

Microalgae cultivation and harvesting. Tetraselmis suecica (UTEX LB2286, University of Texas Culture Collection of Algae, USA) was cultivated using two different systems. For lab-scale experiments, cultivation took place in a 25 L flat panel photo-bioreactor. Ten fluorescent lamps (Philips 58 W/840) provided a continuous incident light of 373 ± 18 μmol m^{-2} s^{-1}. Mixing and pH ~ 7.5 were maintained by sparging gas (0.25 vvm) composed of a mix of air and 5% v/v CO_2. For semi-pilot scale experiments, cultivation was done in a 300 L tubular horizontal photo-bioreactor. The system was subjected to artificial light by 7 halogen lamps with a total incident light of 312 ± 25 μmol m^{-2} s^{-1} and a light:dark regime of 20 h:4h. pH ~ 7 was controlled by sparging a blend of air and 7% (v/v) CO_2 at 0.25 vvm. The culture was thoroughly mixed in a mixing chamber fitted in the system by continuous liquid recirculation at a rate

of 30 L min^{-1}. Both systems are operated under batch mode. Walne medium was supplied at the beginning of the culture at a ratio of 8.8 mL L^{-1} culture (Michels et al., 2014). Temperature was maintained at 20 °C via inner coils controlled by an external cooling unit. The photo-bioreactors were located in a greenhouse in AlgaePARC, Wageningen – The Netherlands. Cultures were harvested by centrifugation (3100*g*) using a spiral plate centrifuge (Evodos 10, Evodos, The Netherlands). After centrifugation, the biomass paste was stored in dark at 4 °C. The experimental data for *Chlorella vulgaris* at laboratory scale was obtained from Postma et al. (2017, 2015). In short, the strain SAG 211-11b (EPSAG Göttingen) was cultivated in repeated batches in a 12 L photobioreactor in M8a-medium. pH was controlled at 7 by supplying air and CO_2 at 0.25 vvm. The incident light intensity was increased from 400 to 1100 μmol m^{-2} s^{-1} during culture time. For pilot experiments, *Chlorella vulgaris* UTEX 2714 was kindly provided by Dr. Dorinde Kleinegris (UniResearch, Bergen-NO) and Jeroen de Vree (University of Bergen, Bergen-NO).

Algae disintegration. Prior to the disintegration experiments, the algae paste was re-suspended in phosphate-buffer saline (PBS: 1.54 mM KH_2PO_4, 2.71 mM $Na_2HPO_4{\cdot}2H_2O$, 155.2 mM NaCl at pH 7.0) to obtain the desired biomass concentration. Disintegration experiments were conducted in batch recirculation mode (Fig. 1A) using two horizontally oriented bead mills (Willy A. Bachofen AG Maschinenfabrik, Muttenz, Switzerland). Laboratory scale studies were conducted in a 0.079 L mill (DYNO-Mill Research Lab). To test the effect of the shear generated by the agitator on the cells, the mill was run without beads at 1500, 3500, and 5500 rpm and slurry concentrations of 30, 93, and 155 g kg_{DW}^{-1}. Additionally, disintegration studies were performed at bead filling ratios of 2.5, 10, 45, 65 and 75%. These correspond to the percentage of the maximum achievable packing. With respect to absolute filling, the filling ratios are 1.6, 6.3, 28.6, 41.2 and 47.6%. Semi-pilot experiments were conducted in a 0.5 L mill (DYNO-Mill Multilab) at 75% bead filling ratio and 1800 rpm. Both milling systems contained 0.5 mm Yttria-stabilised ZrO_2 beads (Tosoh YTZ®). Temperature was controlled at 25 °C by external cooling units fitted to the mill's cooling jacket. Equipment details are given in Table 1.

Power consumption and heat dissipation. Power consumption was estimated from the actual torque and agitator's speed used by the mill during operation. Heat dissipation was assessed by running the mill (65% of 0.5 mm beads, 100 g L^{-1} biomass slurry) without external cooling and by recording the temperature increase over a period of 20 min. The corresponding power was estimated from the temperature increase using as specific heat 3.87 J kg^{-1} K^{-1} and density of 1200 kg m^{-3} (Schneider et al., 2016).

Table 1
Dimensions of bead mills used for the disintegration experiments.

Section	Unit	Laboratory	Semi-pilot
Chamber volume	mL	79.6	500
Chamber radius	mm	29.5	38.5
Accelerator radius	mm	25	31.8
Number of accelerators		1	3
Shaft radius	mm	15	13.3
Chamber length	mm	38.5	139.1
Accelerator length	mm	22	99.1
Shaft length	mm	7	40.0

Sample collection for kinetic studies. For each experiment, samples were collected at different times directly from the feeding chamber (Fig. 1A). The volume of the total samples never surpassed 5% of the feed volume. After collection, samples were centrifuged at 20,000 RCF and 20 °C for 20 min. The supernatants were separated and stored at 4 °C prior to analysis.

Sample analysis. Dry weight was determined gravimetrically after drying for 24 h to constant weight using a Sublimator 2×2×3 (Zirbus technology, GmbH). Analysis of the soluble phase was conducted as described by Postma et al. (2017). In short, protein content was determined following the method of Lowry (Lowry et al., 1951) using Bovine serum albumin as protein standard. Carbohydrates were measured via the phenol-sulfuric acid method (Dubois et al., 1956) using glucose as standard.

Cell sizing and disintegration. Cell size was estimated with a Beckman Coulter Multisizer 3 (Beckman Coulter, Fullerton USA) with a fixed aperture of 50 μm. Samples were diluted with Coulter Isoton® II prior to analysis. The size distribution of microalgae cells shows a peak at ~1–2 μm which corresponds to flagella, cell debris and bacterial contamination. In this study we report only the mean of the second peak, which correlates to intact cells. The disintegration analysis was conducted as presented in our previous publication (Postma et al., 2017) using a flow cytometer (BD Accuri® C6). Samples were diluted with PBS buffer prior to analysis and measured at fluidics rate of 35 μL min^{-1} and a constant volume of 15 μL. Forward scattering data was used to quantify the degree of disintegration over time.

Viscosity. The viscosity of the biomass slurries was determined using a dial reading viscometer Brookfield® LVT (AMETEK. Inc., USA). Measurements were conducted at ambient conditions.

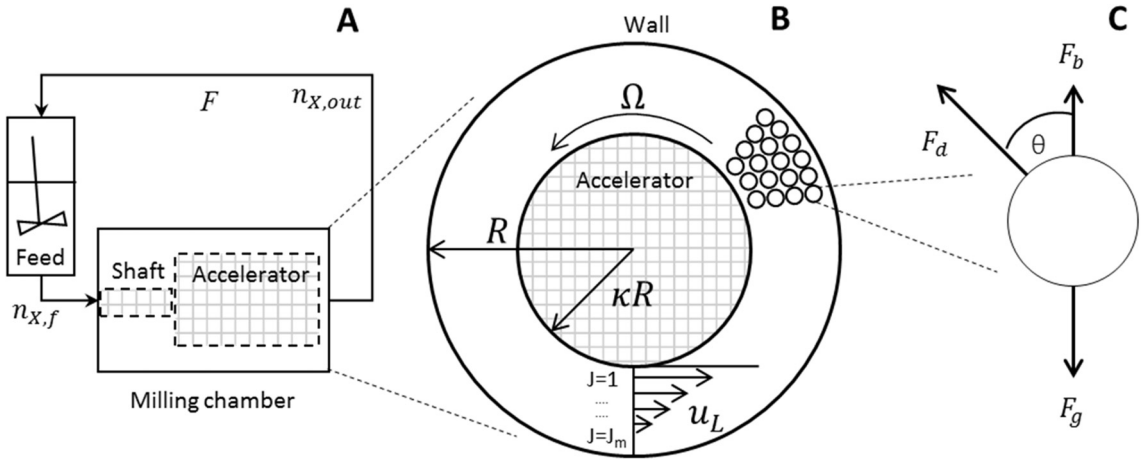

Fig. 1. Schematic representation of the bead milling system. **A:** Milling chamber under batch recirculation mode. **B:** Frontal view of milling chamber with velocity profiles and bead stacking in layers. **C:** Force balance on a single bead (F_d = Drag, F_b = Boyancy, F_g = Gravity).

Statistics. Until otherwise noticed, all experiments were performed in duplicates. Statistical analysis at 95% confidence level was conducted using R (V 3.4.0). Significance was evaluated by applying one way ANOVA. To compare significantly different means, a Tukey's Honest Significant Tests (HSD) was applied.

3. Model development

A schematic representation of the milling system under batch recirculation mode is shown in Fig. 1. A suspension containing alga cells at a concentration n_x is fed from a hopper to the milling chamber via a conveying screw and recirculated back at a constant rate F. In the milling chamber, disintegration takes place as a result of the shear caused by colliding beads. The following assumptions are made:

i. As shown in Fig. 1A, an external stirrer is placed in the feeding hopper and thus, ideally mixed conditions are assumed (Eq. (1)). The conveying screw forces the fluid through the milling chamber where strong mixing takes place, pushing the fluid back to the feed section. Here, ideally mixed conditions are considered (Montalescot et al., 2015) (Eq. (2)):

$$V_f dn_{X,f} = F(n_{X,out} - n_{X,f})dt \tag{1}$$

$$Fn_{X,out} = Fn_{X,f} - n_{X,out}k_D V_{ch} \tag{2}$$

$$V_f = V_{susp} - (1 - \alpha * (1 - \varepsilon))V_{ch} \tag{3}$$

where ε is the porosity of the bead porosity due to packing, V_{ch} is the volume of the mill chamber, α is the bead filling ratio, $n_{X,f}$ and $n_{X,out}$ are the cell concentrations in the feed and mill respectively, and V_f the volume of feed. In Eq. (2), k_D [s^{-1}] is a constant given by:

$$k_D = \frac{V_x}{V_{ch}}\eta\frac{E}{E_X} \tag{4}$$

where V_X is the volume of a single cell, E is the total energy resulting from collisions in the mill and E_X the energy required to break a single cell. The fraction $V_x\, V_{ch}^{-1}$ represents the probability of cells to be hit by collisions in the mill while the fraction $E\, E_X^{-1}$ accounts for the excess of energy of collisions in the mill. While k_D can be seen as a constant accounting for cell death, η represents the "effective disintegration energy" and gives an indication of the energy losses for other purposes rather than cell disintegration.

ii. In the mill chamber, the accelerator rotates at a constant speed ω and transfers momentum to the fluid and to beads of equal size d_b (Fig. 1B). The movement of the beads is governed by several forces, including gravity, drag and buoyancy (Fig. 1C). By applying a force balance on an individual bead, the resultant bead velocity is given by:

$$u_b = u_L\left(1 - \exp\left(-\frac{18\mu}{\rho_b d_b^2}t\right)\right) \tag{5}$$

where u_L and μ are the liquid velocity and viscosity respectively, and ρ_b is the bead density. In Eq. (5) it was assumed that the effects of gravity and buoyancy cancel out at the opposite positions in the circular coordinate. In addition, centrifugal force, hydrodynamic lift, Coriolis force and bead rotation are neglected. This allows us to formulate bead velocity as a function of the frictional force or Stokes' drag (Dogonchi et al., 2015). Eq. (5) predicts that $u_b \approx u_L$ even for very short times due to the small bead size. We therefore assume that the fluid and the beads are traveling at equal speeds. Consequently, u_b is a function of the radial position as there is a distribution of velocities between the accelerator and the chamber wall. Furthermore, we consider beads to be homogeneously distributed in the mill and stacked in layers (Fig. 1B).

iii. The stacking of beads in layers has also been used by Doucha and Lívanský (2008) and allow us to have a distribution of number of beads and their velocities by layers (J to J_m), i.e., there are fewer beads close to the accelerator traveling at maximum speed (speed of the accelerator) and more beads close to the wall moving at low speeds or static. This also means that more layers are available for beads of smaller size. Computational estimations by Yamamoto et al. (2012) support these assumptions.

iv. The alga slurry behaves like a Newtonian fluid. Preliminary experimental data revealed negligible changes in viscosity during bead milling (Supplementary data). Thus, the *Navier-Stokes* equation in *Couette* flow (Bird et al., 2002) can be used to describe the fluid velocity distribution u_L in the annular section (Fig. 1B). The effect of gravity on the flow distribution and the axial velocity component are deemed negligible. Under these conditions, the velocity profile and shear rate ($\dot{\gamma}$) in the mill are given by (Gers et al., 2010; Michels et al., 2016; Yamamoto et al., 2012):

$$u_L = \frac{\Omega\kappa^2}{1-\kappa^2}\left(\frac{R^2}{r} - r\right) \tag{6}$$

$$\dot{\gamma} = \frac{2\Omega\kappa}{1-\kappa^2} \tag{7}$$

where κ is the ratio of the radius of accelerator and mill chamber (R), Ω is the angular velocity and r is the radial position inside the mill. Correspondingly, the shear stress can be estimated by multiplying the shear rate and the fluid viscosity (Bird et al., 2002; Geankoplis, 1993; Michels et al., 2010). Moreover, Eqs. (5) and (6) were applied to the two sections of the milling chamber: shaft and accelerator.

v. The moving beads carry kinetic energy which is released upon collisions. The frequency of collisions per unit volume (z) was estimated according to the kinetic theory of gases (Atkins and Paula, 2006) as proposed by Melendres et al. (1991):

$$z = \frac{\sqrt{2}}{2}u_b\pi d_b^2 n^2 \tag{8}$$

where n is the number density of beads (number of beads per unit volume). Since there is a distribution of velocities for the beads, Eq. (8) leads to a distribution of frequency of collisions as a function of the mill radius.

vi. Several types of interactions can take place among moving beads, including impact, torsion, shearing and rolling (Beinert et al., 2015). Similarly, the interaction of colliding beads and cells can result in shear forces, compressive forces and impact forces (Pan et al., 2017). It was assumed that all the energy is released after single collision impacts and that their energy is equivalent to the kinetic energy carried by the beads:

$$E_b = \rho_b V_b u_b^2 \tag{9}$$

where ρ_b and V_b are the density and volume of the bead, respectively. The total energy released by colliding beads (E) is therefore calculated as the product of the energy and frequency of collisions (Kwade and Schwedes, 2002):

$$E = \sum_{j=1}^{jm} E_{b,j} * z_j * V_j \tag{10}$$

where the subscript j refers to the radial stream layers in which the beads are moving in the milling chamber (Fig. 1B).

vii. The specific disintegration energy E_X depends on the physiological structure of each species and on the media osmolality. The corresponding values for *T. suecica* (17.4 pJ) and *C. vulgaris* (22.8 pJ) were taken from Lee et al. (2013) and Günther et al. (2016) and corrected by the osmolality of the media (PBS buffer). Although cell

disintegration can also take place as a result of cumulative damage, such effects were not taken into consideration. This is because of the lack of knowledge regarding the effect of every shear event on the cell structure, and how they contribute to lowering the cell-wall strength and to the disintegration process.

viii. Several authors have recognized the existence of a region between colliding beads in which disintegration effectively takes place (Bunge et al., 1992; Kwade and Schwedes, 2002; Melendres et al., 1991). We have introduced the concept of "effective disintegration energy" η to account for the energy released after collisions that reache the cells to cause damage or disintegration. Suarez Garcia et al. (2018) presented an overview of the specific energy consumption (E_m) of several bead milling processes reported in literature for microalgae disintergation; the average experimental value was $E_{m,\exp} = 11.8$ kWh kg_{DW}^{-1}. On the other hand, the average experimental energy for disintegration is $E_x = 1.35 \times 10^{-3}$ kWh kg_{DW}^{-1}. η was therefore calculated as $\eta = E_X/E_{m,Exp} = 1.15 \times 10^{-4}$.

Eqs. (1) and (2) can be solved in order to estimate the amount of cells that are leaving the milling chamber $n_{x,out}$:

$$\frac{dn_{X,out}}{dt} = -k_{dis} n_{X,out}; k_{dis} = \frac{F}{V_f}\left(\frac{F}{F + k_D V_{ch}} - 1\right) \quad (11)$$

Eq. (11) corresponds to a first-order kinetic model, as several authors have implemented to describe the disintegration kinetics of bacteria, yeast and microalgae in bead mills (Doucha and Lívanský, 2008; Kula and Schütte, 1987; Middelberg, 1995; Zinkoné et al., 2018).

Model solution. The values of k_{dis} for several experimental and processing conditions were estimated by solving Eqs. (3)–(11) using Matlab® R2015b.

4. Results and discussion

Cell damage and disintegration occur as a result of the cumulative intensity of the forces that effectively reach the cells. The nature of such forces and their effect on the cells depend on the type of disintegration method. In general, differences in osmotic pressure, electric fields, eddy diffusion, turbulence, cavitation, hot spots and/or shear caused by mechanical elements are believed to be the responsible mechanisms of damage on the cell structure (Brookman, 1974). The rigidity of the cell envelope also plays a critical role to withstand shear forces, temperature or extreme local pressure gradients. Cell strength varies greatly depending on the microalgae strain and the cell physiology. Wang and Lan (2018) reported critical stress values (i.e., pressure limit to ensure cell viability) for several algae species in the range 1.6×10^{-4} to 88 Pa. Low critical values are often occurring in strains displaying outer peptidoglycan layers, plasma membranes or polysaccharides which can dissolve in the culture medium (Geresh et al., 2002). On the contrary, strains with a cell wall rich in polymers like cellulose or sporopollenin (Hagen et al., 2016), are highly resistant to stress and chemical treatments. *Tetraselmis suecica's* cell wall rich in a pectin-like polysaccharide (Kermanshahi-pour et al., 2014), which confers the cells relative resistance to shear stress (Michels et al., 2016). *Chlorella vulgaris* is believed to contain a cell wall rich in cellulose and hemicellulose (Abo-Shady et al., 1993) and therefore displays a greater resistance against external stress. In a milling chamber, however, shear can be originated from collisions, from friction between beads or from the turbulence generated nearby the accelerator or close to the wall. Several experiments were therefore conducted in order to assess the effect of shear caused by agitation without beads.

4.1. Effect of shear on cell disintegration

The shear generated by the rotation of the agitator without beads, in the range 1500–5500 rpm, has a negligible effect on the cells of *T. suecica*. This was confirmed by measuring the percentage of cell disintegration and the amount of released proteins and carbohydrates after 20 min of operation. As presented in Fig. 2A, cells remain practically intact and the amount of released biomolecules varies only marginally ($p > 0.05$). Even after 1 h of operation, no significant effect was noted (data not shown). Under these operational conditions, the alga cells were exposed to theoretical shear stress up to 5.5 kPa (Eq. (7)), which is well above the critical stress level of 88 Pa reported by Michels et al. (2016). Lee et al. (2013) reported a minimum experimental force required to disrupt a cell of *T. suecica* of 7.1 ± 3.5 μN. By considering this force acting on the surface of a cell with an average diameter of 7 μm, the minimum theoretical stress required to cause disintegration varies from 23.4 to 68.8 kPa. This confirms that agitation alone is insufficient to induce cell disintegration or release of proteins and carbohydrates from the alga under study.

Simulations of the fluid and bead flow profiles were conducted at agitation speeds of 1500–5500 rpm, bead sizes of 0.3–1 mm and fluid viscosities of 1×10^{-3} to 1.6 Pa s. This range of viscosities was determined during preliminary experiments (data not shown), as it covers the biomass concentrations typically reported in literature. It was found that the flow profile for the beads deviates significantly from the ideal *Couette* flow (Eq. (6)) only at low viscosity values ($\mu < 0.01$ Pa s) and short times ($t < 0.1$ s). Since all disintegration experiments were conducted with biomass slurries displaying viscosities above 0.017 Pa s, significant differences in

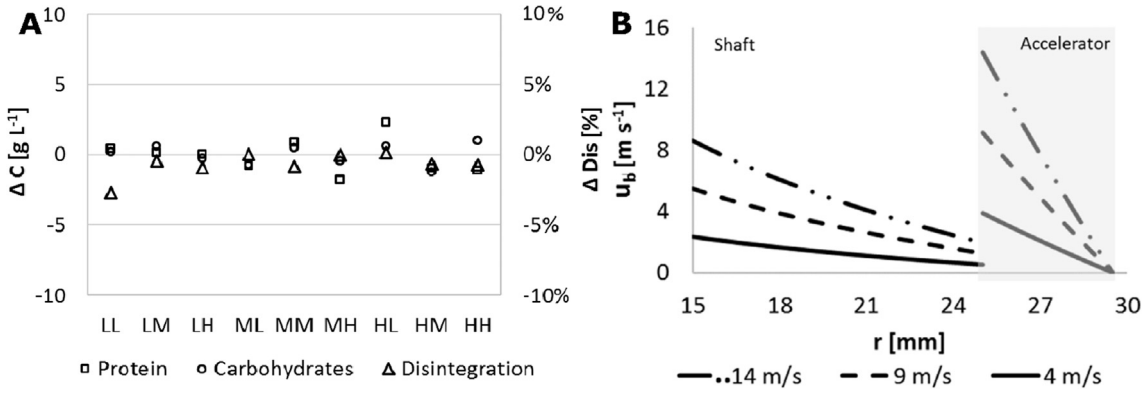

Fig. 2. A. Variation in the percentage of disintegrated cells and released proteins and carbohydrates after 20 min stirring without beads. Letters in the y-axis refer to the operating conditions (L: Low, M: Medium, H: High) for biomass concentration: 30, 93, 155 g L^{-1}, and agitation: 1500, 3500, 5500 rpm. **B.** velocity profiles of beads in the milling chamber at several tip speeds [m s^{-1}].

fluid and bead velocity are only taking place at $t < 0.05$ s. It is therefore assumed that $u_b = u_L$. It is worth noticing that in reality the flow patterns in agitated mills is greatly complex (Blecher et al., 1996) and depends on several variables. Our oversimplification, however, makes possible to have an estimate of the velocity profiles which is used to calculate the energy released from the colliding beads.

The bead velocity profiles developed in the milling chamber at several agitation speeds in both the shaft and accelerator regions are shown in Fig. 2B. The simulations show that the beads acquire the tip velocity in the vicinity of the shaft or accelerator, and become nearly static at the chamber's wall. As expected, beads reach a higher speed over the accelerator where maximum energy densities are expected. Computational simulations conducted by Yamamoto et al. (2012) on horizontally oriented mills confirm our simulations: beads nearby the agitator move at maximum speeds while a larger number of beads are located around the proximity of the wall, moving at low speeds or almost static. Within the range of experimental conditions tested in the present study for cell disintegration, the Reynolds number (Eq. (12)) varies in the interval $1 \times 10^3 \leq Re \leq 9 \times 10^3$ which corresponds to the Doubly periodic flow regime (Bird et al., 2002). This is a complex flow regime involving periodic waves traveling in the tangential direction. Only for slurries with a viscosity of 1.6 Pa s, $Re \approx 100$, under which laminar flow can be considered. As the description of the flow under the actual regime is overly complex or unknown, the simplification to laminar regime is required.

$$Re = \Omega \rho_L (\kappa R)^2 \mu_L^{-1} \tag{12}$$

4.2. Power consumption in the milling chamber

Experimental evidence indicated that shear from the accelerator alone -without beads- is not responsible for cell damage or disintegration during bead milling. In this regard, cell rupture takes place as a result of the energy released by colliding beads and depends on the probability of cells to be trapped in between colliding beads, where shear is strong enough to cause disintegration (Kula and Schütte, 1987). To further understand the energy distribution in the mill and its effect on cell disintegration, the power consumption of the laboratory scale mill under several conditions was measured and the results compared in Fig. 3A.

As can be seen, for a stirring speed of 1500 rpm, the power consumption remains practically stable even if the mill runs empty or with beads (65%) and biomass slurry (155 g L^{-1}). The corresponding measured heat dissipation at this speed reaches 17.8% of the total power spent. The power consumption further increases following an exponential tendency as the agitation speed augments to 3500 and 5500 rpm. This can be the result of the chaotic movement of the beads which forces the accelerator to demand higher power in order to keep a constant stirring speed. Under 3500 and 5500 rpm, the measured power dissipated as heat reaches 24.2% and 60.8% of the total respectively, confirming excessive shear generation. Furthermore, the simulations indicate that approximately 95% of the total energy released from collisions in the mill is occurring in the region of the accelerator. This suggests the existence of a zone of high energy surrounding the accelerator and a zone of low energy located around the shaft and close to the wall. In Fig. 3B the theoretical energy released as a result of collisions over the accelerator is plotted against the annular gap for several bead sizes and a constant stirring speed of 3500 rpm ($Re \approx 5000$). At the vicinity of the accelerator, there is a high energy density which falls exponentially near the wall. Blecher et al. (1996) also proposed an energy density distribution in agitated mills which is mainly determined by the velocity gradients of the fluid. Their simulations, however, predicted the existence of two high energy zones: close to the agitator disc and close to the wall. Similarly to our predictions, the regions of high energy account for about 90% of the total energy dissipated in the mill.

4.3. Simulation of disintegration rates

Experimental data and simulations show that colliding beads are required to cause cell disintegration and that the region surrounding the accelerator accounts for almost all (90%) the energy released in the milling chamber. This energy is used to calculate the disintegration kinetics constants (k_{dis}) according to Eq. (11). The simulated k_{dis} as a function of the accelerator's tip speed, cell size and cell strength are displayed in Fig. 4. As expected, the disintegration rates decrease as the cell strength, in terms of minimum energy required for disintegration, increments from 5 to 80 pJ. This range covers a broad range of microorganisms and algae strains. For instance, the force required to break mammalian cells ranges from 1.5 to 4.5 μN (Mashmoushy et al., 1998), while for bacteria and yeast the ranges are 3–34 μN (Shiu et al., 2002) and 55–175 μN (Mashmoushy et al., 1998) respectively. *T. suecica* demands a force of 7.4 μN (Lee et al., 2013) whereas for *C. vulgaris*, the force can increase 5 fold for high medium osmolality which directly affects the cell's turgor pressure (Günther et al., 2016).

From Fig. 4. it is also clear that Eq. (11) predicts an increment in k_{dis} as the cell size or the tip speed increases. This means that larger cells are more likely to be trapped in between colliding cells, which will result in higher degrees of disintegration. Similarly, at larger

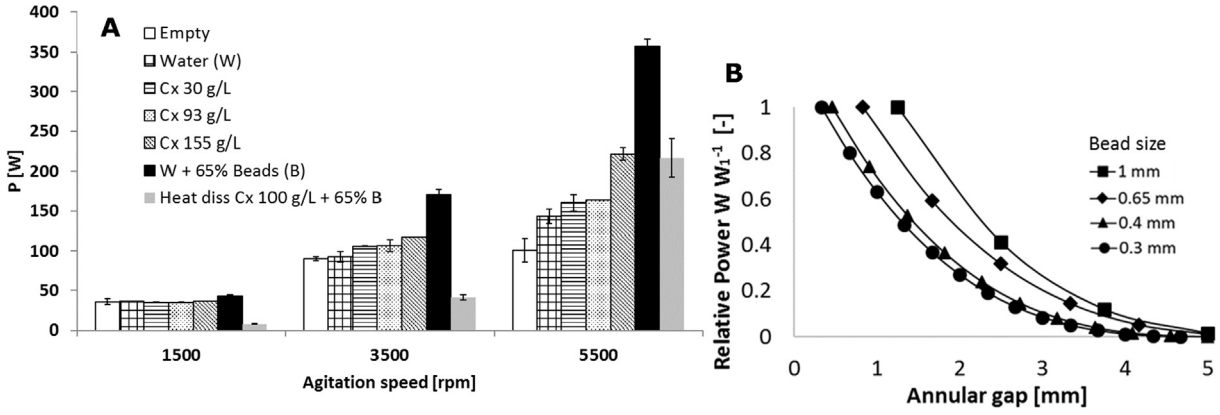

Fig. 3. A. Power consumption for the laboratory scale mill under several processing conditions. **B.** Theoretical power released by colliding beads over the annular for different bead sizes.

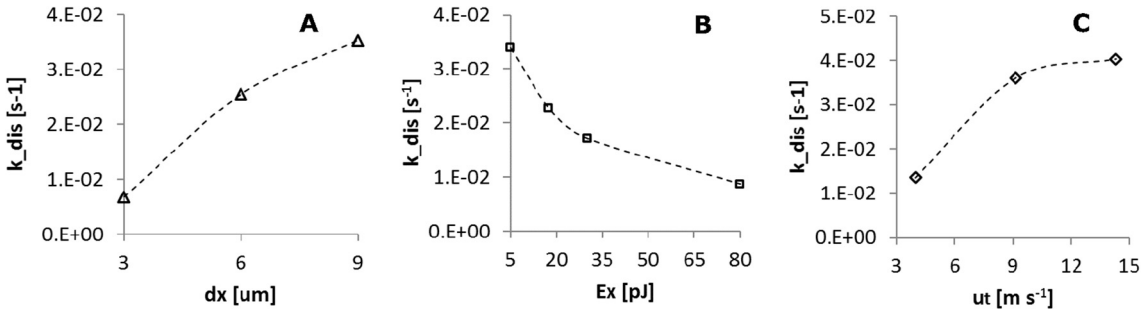

Fig. 4. Predicted disintegration rates k_{dis} [s^{-1}] at fixed bead size (0.5 mm) and bead filling (65%) as function of cell size (d_X) **(A)**, cell strength (E_X) **(B)** and tip speed (u_t) **(C)**. The standard value of the parameters are u_t = 6.8 m s^{-1}, E_X = 17.4 pJ and d_X = 6 um.

agitation speeds both the frequency and intensity of collisions are higher and so does the energy available for disintegration. Tip speed, however, appears to have a marginal effect on k_{dis} above 3500 rpm (u_t > 9.6 m s^{-1}). This resembles what Kwade and Schwedes (2002) defined as optimal stress intensity (SI_{opt}), a limit above which an additional energy input has a negligible effect on the comminution process. As also observed in Fig. 3A, heat dissipation becomes excessive beyond 3500 rpm, which will have an impact on product quality and operation costs. The model predictions can therefore serve to establish a window of operation to maximize disintegration and reduce costs. The tendencies simulated for d_X vs k_{dis} (Fig. 4) were experimentally observed by Zinkoné et al. (2018) and Montalescot et al. (2015) on a continuously operated bead mill for several algae strains of sizes ranging from 3 to 9 μm. The authors indicated that bigger cells, are disintegrated more rapidly as the probability of larger cells to be trapped in between colliding beads is higher. The influence of cell strength was, however, not assessed. Postma et al. (2017) also reported k_{dis} for three different algae strains of sizes ranging from 3.1 to 7.6 μm. Similar observations were made, but the results were explained considering differences in cell strength rather than on cell size. To our knowledge, the present study is the first attempt to incorporate cell strength to predict disintegration rates for microalgae in bead mills.

4.4. Model validation

Model predictions as given by Eq. (11) were validated against experimental data collected in this investigation along with data published by Postma et al. (2015) and Postma et al. (2017). In all cases, the same bead mill and operation mode were used. In Fig. 5, the kinetic constants reported by Postma et al. (2015) for the disintegration of *C. vulgaris* as a function of tip speed (u_t) and biomass concentration (C_X) are compared against the model estimations. The model predicts that k_{dis} increases at higher u_t, which is due to a higher kinetic energy delivered by the colliding beads, and remains practically stable at various C_X. In this regard, the published data is contradictory and appears to depend on the system under investigation. Some studies find a positive effect of C_X on k_{dis} while others report an optimal, negative or negligible effect for algae and yeast (Doucha and Lívanský, 2008; Montalescot et al., 2015). It appears that biomass concentration is important mainly to ensure low specific energy consumptions.

The data from Postma et al. (2015) show a slight increase of k_{dis} as function of u_t,. Considering the uncertainty associated with the experimental data (≈21%) the model shows acceptable predictions, except at u_t = 12 m s^{-1} where deviations are significant. This suggests that the energy dissipated at high agitation rates is larger in practice than estimated in the model and thus, it indicates that a smaller value of η is needed for such conditions.

Bead size and bead filling are crucial parameters since they are directly related to the total energy that can be released in the milling chamber. Several investigations have addressed the influence of bead size on the k_{dis} of algae in bead mills. Higher disintegration extents have been reported for the microalgae *Scedenesmus* sp., *Nannochloropsis oculata*, and *Chlorella sorokiniana* as the bead size decreases, in particular for beads in the range 0.2–0.6 mm (Hedenskog et al., 1969; Montalescot et al., 2015; Zinkoné et al., 2018). The bead material has also a direct effect on the disintegration of algal cells (Montalescot et al., 2015). It has been reported that larger disintegration levels are obtained with zirconia beads in comparison to glass beads probably due to their higher density which results in enhanced kinetic energy at constant speeds (Doucha and Lívanský, 2008). In Fig. 6A-B, the corresponding k_{dis} for two algal strains reported by Postma et al. (2017) using zirconia beads at 65% filling rate are compared with the model calculations. The model accurately predicts the trends for *T. suecica* (Fig. 6A) and *C. vulgaris* (Fig. 6B). For the former, no significant variation of k_{dis} was obtained at different values of d_b. This can be explained by its relatively weak cell wall which can be disintegrated at

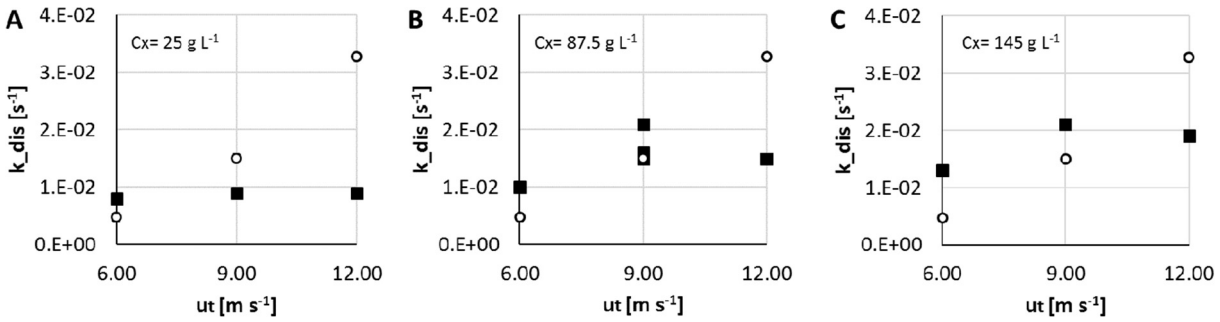

Fig. 5. Comparison of model predictions (o) with data published by Postma et al. (2015) (■) for *C. vulgaris*. Graphs **A**, **B** and **C** show k_{dis} vs u_t at initial biomass concentrations of 25, 87.5 and 145 g L^{-1} respectively.

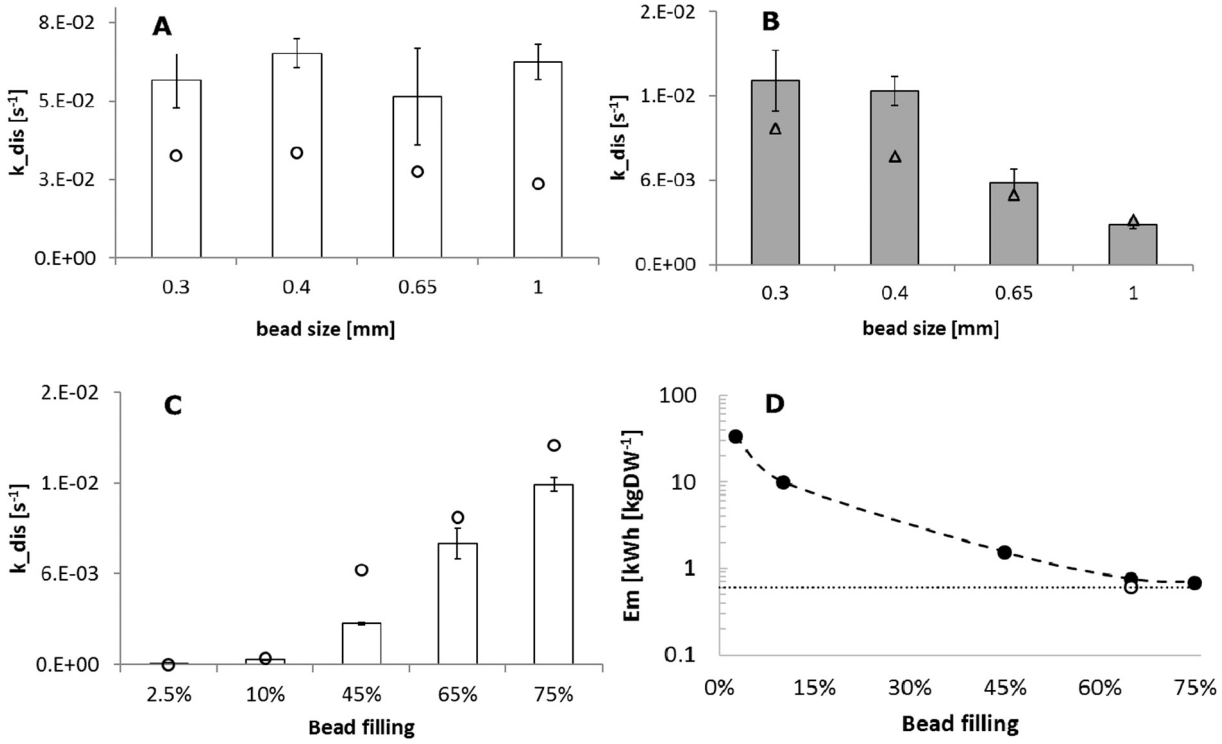

Fig. 6. **(A-B)** Disintegration rates for two algae strains at different bead sizes. Experimental data from Postma et al. (2017). **A.** *T. suecica* (o). **B.** *C. vulgaris* (Δ). **C.** Disintegration rates at different bead fillings for *T. suecica* (o). Columns: experimental data. Markers: model predictions. **D.** Specific energy consumption (E_m, Log scale) as function of the bead filling to reach 95% cell disintegration. Open marker: Experimental data (Suarez Garcia et al., 2018). Dotted line: E_m for extraction (Coons et al., 2014).

comparable rates regardless of the bead size. For *C. vulgaris*, the model captures the general expected behaviour: k_{dis} decreases as the bead size increases, confirming previous studies (Postma et al., 2017). Although with smaller beads the kinetic energy carried per bead is lower, the number of beads and therefore number of collisions that take place in the milling chamber is higher, suggesting that the frequency and not intensity of the collisions is the rate controlling factor during bead milling. Zinkoné et al. (2018) found a linear correlation of stress frequency with k_{dis} for *C. sorokiniana* in a continuously operated bead mill. Stress frequency is defined as the number of stress events per unit time (Kwade, 1999).

The effect of bead filling (α) on the disintegration of algal cells is often overlooked. Montalescot et al. (2015) evaluated disintegration rates for *P. cruentum* from 35 to 65% and Doucha and Lívanský (2008) presented data for several milling systems in the range 60–85 %. In both cases, it was reported higher disintegration rates at higher α. In Fig. 6C, experimental data and model results for *T. suecica* at α from 2.5 to 75% are shown. The predicted data accurately describe the experimental values, reflecting that as α increases, the number of beads and the frequency of collision becomes larger, therefore disrupting more cells per unit time. At low α, the frequency of collisions is low, requiring remarkably long residence times to achieve complete cell disintegration. This, in turn, implies large equipment volumes and consequently high capital expenses. As the value of α increases, the energy released by colliding beads becomes larger, and complete disintegration is obtained in short times. The corresponding specific energy consumption to reach 95% disintegration (E_m) as function of the bead filling is presented in Fig. 6D. As shown, E_m decreases mainly due to the impact of bead filling on residence time, as 95% disintegration is reached faster at high α. Furthermore, as the data presented in Fig. 6D was collected at moderate agitation speeds (2039 rpm), it is expected that no significant additional power will be consumed as a result of the presence of the beads (Fig. 3A). Operating the mill at α = 65–75% will guarantee that the target for energy consumption for the extraction step within an algae biofuel biorefinery $E_{m,Extr}$ = 0.6 kWh kgDW^{-1} (Coons et al., 2014) is achievable.

The development of mild and energy efficient disintegration processes is crucial to ensuring the extraction of functional biomolecules from algae and to realise algae-based processes at large scale (Suarez Garcia et al., 2018). In this regard, the modelling approach presented in this investigation allows the study of the disintegration of several microalgae species when information on the cell-wall strength and size are known. Moreover, the model makes possible the selection of an operational window depending on the biorefinery needs. Agitation speed, bead filling, bead size and flow rate can be estimated to target specific groups of cells within a population. For example, cells that accumulate preferentially a metabolite of interest and therefore appear larger (Cabanelas et al., 2016) or cells displaying a stiffer cell-wall because they are undergoing a different stage in the cell cycle as demonstrated by de Winter et al. (2013), cells accumulate first proteins and pigments and later carbohydrates and lipids during the growth phase of synchronized cultures. This can be exploited in order to release selectively metabolites during bead milling and to obtain crude fractions with higher purities. Also, in case of a mixed algae population, the operational parameters of the mill can be tuned to operate within a range of energy values (energy released in the milling chamber) to selectively release high-value biomolecules that are produced by a certain strain only. More extensive knowledge on the cell-wall composition and the energy required to disrupt a single cell is therefore needed (Alhattab et al., 2018).

4.5. Effective disintegration energy

We have introduced the term effective disintegration energy η as a factor that indicates the fraction of energy that is dissipated into the medium, without effectively reaching the cells. A

significant portion of the total available energy is spent in providing momentum to the mechanical elements of the mill as well as to the biomass slurry and the beads. It was determined that as the agitation speed increases, the energy demand and heat dissipation becomes significant (Fig. 3A), which is probably due to the complex nature of the collisions occurring in the mill. We have assumed perfectly elastic collisions occurring at a frequency similar to that of gas molecules. In this case, molecules collide in a constant, rapid, random motion, which can also take place with beads in the milling chamber.

However, the real nature of the collisions, flow regimes and the actual gradients of speeds at which collisions are taking place are unknown (Becker et al., 2001). For instance, the coefficients of friction and restitution (Beinert et al., 2015), which determine the velocity of the beads upon collision, have not been taken into consideration. For the estimation of the collision frequency, the kinetic theory of gases was used, but this requires particles with negligible volume, which does not hold for the system under study, in particular at high filling ratios. The values of E_X were taken from studies in which nano-indentation was used. However, during bead milling, the beads have a typical diameter of 10^2-fold larger than the cell diameter. Since the contact area provided by the needle during indentation is much smaller than the area of a bead in contact with a cell, a stronger force is needed from the beads to attain the same pressure. Also, there are physiological variations for the same strain due to culture conditions and random mutagenesis, which have a direct effect on the values of E_X.

4.6. Selective release of biomolecules

The comminution process of microorganisms cannot be defined by the fineness of the cell debris but from the cell rupture and consequent release of biomolecules into the surrounding fluid. In this regard, cell disintegration and release of biomolecules are proportionally correlated. We analysed the experimental data reported by Postma et al. (2017) for the release of proteins and carbohydrates from three microalgae species and found that protein and carbohydrate release can be estimated directly from the rates of disintegration. In other words, with a confidence level of 95%, the rates of proteins and carbohydrate release are proportional to k_{dis}. The rates of pigment release also appear to be dependent on k_{dis} as pigments are normally located in the chloroplast or in internal storage organelles (de Winter et al., 2013; Suarez Garcia et al., 2018). Therefore, the accurate estimation of the disintegration rates not only provides crucial information for the design and optimization of the disintegration processes, but also for the fractionation and purification steps downstream. A clear example of this is that differences in the rates of disintegration and release can be exploited to selectively enrich the extract phase with a metabolite of interest, which can favour both the yields and purities (Suarez Garcia et al., 2018).

4.7. Scale-up

The predictive capabilities of Eq. (11) were also evaluated for a system at semi-pilot scale as described in Section 2 and Table 1. The experimental disintegration rate for *T. suecica* was $1.29 \pm 0.08 \times 10^{-2}$ s^{-1} and that for *C. vulgaris* was $4.14 \pm 0.09 \times 10^{-3}$ s^{-1}. The simulated rates were 7.86×10^{-3} s^{-1} and 3.58×10^{-3} s^{-1} respectively. The corresponding kinetic curves are shown in Fig. 7. As expected, higher disintegration rates are obtained for *T. suecica* as its cell wall is weaker and thus, the energy released in the bead mill is sufficient to break more cells per unit time. The model presented in this investigation can potentially be used for scale-up purposes. By keeping the rates of disintegration k_{dis} uniform at different scales, the model can be solved to estimate the corresponding rotational speeds, bead size, bead filling and geometrical dimensions of the mill at a larger scale. This can be made strain-dependent or can be aimed at multi-strain and multiproduct biorefinery process. Such scale-up procedure can be considered as a combination of rate of production, and sizing by energy (Austin, 1973), since it involves equating k_{dis} for two scales and incorporating the energy consumption as function of operational parameters.

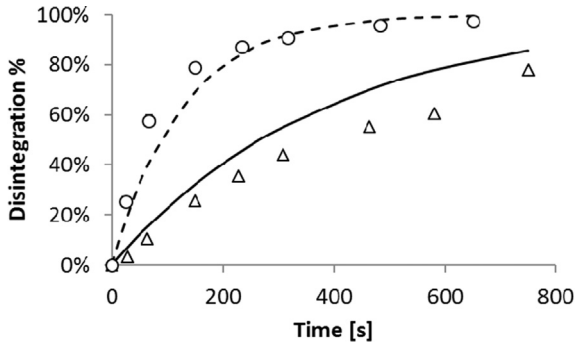

Fig. 7. Disintegration profiles for *T. suecica* (o) and *C. vulgaris* (Δ) for a semi-pilot scale bead mill. Dashed and solid lines are model predictions for the respective strains.

Equipment design and optimization studies can also be conducted by solving the model to reach a particular range of values of k_{dis} and determining the values of operational parameters and equipment dimensions. This will ensure not only precise rates of disintegration and release of biomolecules, but also minimum levels of energy consumption and costs. By controlling the disintegration times, it is possible to modify the overall composition of the resulting algae extracts, their properties and their market potential (Suarez Garcia et al., 2018). The applicability of the model is limited by the major assumptions made in terms of hydrodynamics and mechanism of bead collision. However, it can be made extensive to other microalgal cells if information on the size and cell strength is readily available. In other words, the modelling approach presented in this report can find application in multi-feed multi-product microalgae biorefineries.

5. Conclusions

The disintegration of microalgae in bead mills have been studied by means of a modelling approach that involves process and equipment parameters to estimate the theoretical energy released in the mill, and cell parameters to account for the energy needed to disrupt a cell. This allowed us to accurately predict the rates of disintegration of two microalgae species over a broad range of bead sizes and bead fillings, and for two different bead mill scales. Furthermore, we propose that such modelling approach can support development, optimization and scale-up studies and can allow the determination of operation windows to achieve energy efficient, selective and mild disintegration processes for the biorefinery of microalgae.

Declaration of interest

None.

Acknowledgements

This study was financed by the Dutch Technology Foundation STW under the project AlgaePro4You, nr. 12635. From January 2017, STW continued its activities as NWO (Dutch national science

foundation) Applied and Engineering Sciences (TTW). The authors are grateful to Dorinde Kleinegris (UniResearch Bergen, Norway) and Jeroen de Vree (University of Bergen, Norway) for providing *Chlorella vulgaris* for the disintegration experiments.

Appendix A. Supplementary material

Supplementary data to this article can be found online at https://doi.org/10.1016/j.ces.2019.04.008.

References

Abo-Shady, A.M., Mohamed, Y.A., Lasheen, T., 1993. Chemical composition of the cell wall in some green algae species. Biol. Plant. 35, 629–632. https://doi.org/10.1007/BF02928041.

Adarme-vega, T.C., Lim, D.K.Y., Timmins, M., Vernen, F., Li, Y., Schenk, P.M., 2012. Microalgal biofactories : a promising approach towards sustainable omega-3 fatty acid production. Microb. Cell Fact. 11, 1. https://doi.org/10.1186/1475-2859-11-96.

Alhattab, M., Kermanshahi-Pour, A., Brooks, M.S.L., 2018. Microalgae disruption techniques for product recovery: influence of cell wall composition. J. Appl. Phycol. 1, 1–28. https://doi.org/10.1007/s10811-018-1560-9.

Atkins, P., Paula, J., 2006. Physical Chemistry. Oxford University Press.

Austin, L., 1973. Understanding ball mill sizing. Ind. Eng. Chem. Process Des. 12, 121–129. https://doi.org/10.1021/i260046a001.

Becker, M., Kwade, A., Schwedes, J., 2001. Stress intensity in stirred media mills and its effect on specific energy requirement. Int. J. Miner. Process. 61, 189–208. https://doi.org/10.1016/S0301-7516(00)00037-5.

Beinert, S., Fragnière, G., Schilde, C., Kwade, A., 2015. Analysis and modelling of bead contacts in wet-operating stirred media and planetary ball mills with CFD-DEM simulations. Chem. Eng. Sci. 134, 648–662. https://doi.org/10.1016/j.ces.2015.05.063.

Bird, R.B., Stewart, W.E., Lightfoot, E.N., 2002. Transport Phenomena. John Wiley & Sons.

Blecher, L., Kwade, A., Schwedes, J., 1996. Motion and stress intensity of grinding beads in a stirred media mill. Part 1: Energy density distribution and motion of single grinding beads. Powder Technol. 86, 59–68. https://doi.org/10.1016/0032-5910(95)03038-7.

Brookman, J., 1974. Mechanism of cell disintegration in a high pressure homogenizer. Biotechnol. Bioeng. 16, 371–383. https://doi.org/10.1002/bit.260160307.

Bunge, F., Pietzsch, M., Müller, R., Syldatk, C., 1992. Mechanical disruption of Arthrobacter sp. DSM 3747 in stirred ball mills for the release of hydantoin-cleaving enzymes. Chem. Eng. Sci. 47, 225–232. https://doi.org/10.1016/0009-2509(92)80216-Y.

Cabanelas, I.T.D., Van Der Zwart, M., Kleinegris, D.M.M., Wijffels, R.H., Barbosa, M.J., 2016. Sorting cells of the microalga Chlorococcum littorale with increased triacylglycerol productivity. Biotechnol. Biofuels 9, 1–12. https://doi.org/10.1186/s13068-016-0595-x.

Chen, C.Y., Zhao, X.Q., Yen, H.W., Ho, S.H., Cheng, C.L., Lee, D.J., Bai, F.W., Chang, J.S., 2013. Microalgae-based carbohydrates for biofuel production. Biochem. Eng. J. 78, 1–10. https://doi.org/10.1016/j.bej.2013.03.006.

Coons, J.E., Kalb, D.M., Dale, T., Marrone, B.L., 2014. Getting to low-cost algal biofuels: a monograph on conventional and cutting-edge harvesting and extraction technologies. Algal Res. 6, 250–270. https://doi.org/10.1016/j.algal.2014.08.005.

Cuellar-Bermudez, S.P., Aguilar-Hernandez, I., Cardenas-Chavez, D.L., Ornelas-Soto, N., Romero-Ogawa, M.A., Parra-Saldivar, R., 2015. Extraction and purification of high-value metabolites from microalgae: essential lipids, astaxanthin and phycobiliproteins. Microb. Biotechnol. 8, 190–209. https://doi.org/10.1111/1751-7915.12167.

de Winter, L., Klok, A.J., Cuaresma Franco, M., Barbosa, M.J., Wijffels, R.H., 2013. The synchronized cell cycle of Neochloris oleoabundans and its influence on biomass composition under constant light conditions. Algal Res. 2, 313–320. https://doi.org/10.1016/j.algal.2013.09.001.

Dixon, C., Wilken, L.R., 2018. Green microalgae biomolecule separations and recovery. Bioresour. Bioprocess. 5. https://doi.org/10.1186/s40643-018-0199-3.

Dogonchi, A.S., Hatami, M., Domairry, G., 2015. Motion analysis of a spherical solid particle in plane Couette Newtonian fluid flow. Powder Technol. 274, 186–192. https://doi.org/10.1016/j.powtec.2015.01.018.

Doucha, J., Lívanský, K., 2008. Influence of processing parameters on disintegration of Chlorella cells in various types of homogenizers. Appl. Microbiol. Biotechnol. 81, 431–440. https://doi.org/10.1007/s00253-008-1660-6.

Draaisma, R.B., Wijffels, R.H., Slegers, P.M., Brentner, L.B., Roy, A., Barbosa, M.J., 2013. Food commodities from microalgae. Curr. Opin. Biotechnol. 24, 169–177. https://doi.org/10.1016/j.copbio.2012.09.012.

Dubois, M., Gilles, K.A., Hamilton, J.K., Rebers, P.A., Smith, F., 1956. Colorimetric method for determination of sugars and related substances. Anal. Chem. 28, 350–356.

Geankoplis, C.J., 1993. Transport Processes and Unit Operation. Prentice Hall.

Geresh, S., Mamontov, A., Weinstein, J., 2002. Sulfation of extracellular polysaccharides of red microalgae: preparation, characterization and properties. J. Biochem. Biophys. Methods 50, 179–187. https://doi.org/10.1016/S0165-022X(01)00185-3.

Gers, R., Climent, E., Legendre, D., Anne-Archard, D., Frances, C., 2010. Numerical modelling of grinding in a stirred media mill: hydrodynamics and collision characteristics. Chem. Eng. Sci. 65, 2052–2064. https://doi.org/10.1016/j.ces.2009.12.003.

Günerken, E., D'Hondt, E., Eppink, M.H.M., Garcia-Gonzalez, L., Elst, K., Wijffels, R.H., 2015. Cell disruption for microalgae biorefineries. Biotechnol. Adv. 33, 243–260. https://doi.org/10.1016/j.biotechadv.2015.01.008.

Günther, S., Gernat, D., Overbeck, A., Kampen, I., Kwade, A., 2016. Micromechanical properties and energy requirements of microalgae Chlorella vulgaris for cell disruption. Chem. Eng. Technol. 39, 1693–1699. https://doi.org/10.1002/ceat.201400632.

Hagen, C., Siegmund, S., Braune, W., 2016. Ultrastructural and chemical changes in the cell wall of Haematococcus pluvialis (Volvocales, Chlorophyta) during aplanospore formation Ultrastructural and chemical changes in the cell wall of Haematococcus pluvialis (Volvocales, Chlorophyta) during 0262. http://doi.org/10.1017/S0967026202003669.

Hedenskog, G., Enebo, L., Vendlová, J., Prokeš, B., 1969. Investigation of some methods for increasing the digestibility *in vitro* of microalgae. Biotechnol. Bioeng. 11, 37–51. https://doi.org/10.1002/bit.260110104.

Kermanshahi-pour, A., Sommer, T.J., Anastas, P.T., Zimmerman, J.B., 2014. Enzymatic and acid hydrolysis of Tetraselmis suecica for polysaccharide characterization. Bioresour. Technol. 173, 415–421. https://doi.org/10.1016/j.biortech.2014.09.048.

Kula, M.-R., Schütte, H., 1987. Purification of proteins and the disruption of microbial cells. Biotechnol. Prog. 3, 31–42. https://doi.org/10.1002/btpr.5420030107.

Kwade, A., 1999. Determination of the most important grinding mechanism in stirred media mills by calculating stress intensity and stress number. Powder Technol. 105, 382–388. https://doi.org/10.1016/S0032-5910(99)00162-X.

Kwade, A., Blecher, L., Schwedes, J., 1996. Motion and stress intensity of grinding beads in a stirred media mill. Part 2: Stress intensity and its effect on comminution. Powder Technol. 86, 69–76. https://doi.org/10.1016/0032-5910(95)03039-5.

Kwade, A., Schwedes, J., 2002. Breaking characteristics of different materials and their effect on stress intensity and stress number in stirred media mills. Powder Technol. 122, 109–121. https://doi.org/10.1016/S0032-5910(01)00406-5.

Lee, A.K., Lewis, D.M., Ashman, P.J., 2013. Force and energy requirement for microalgal cell disruption: an atomic force microscope evaluation. Bioresour. Technol. 128, 199–206. https://doi.org/10.1016/j.biortech.2012.10.032.

Lowry, O., Rosebrough, N., Farr, L., Randall, R., 1951. Protein measurement with the folin phenol reagent. J. Biol. Chem. 193, 265–275.

Mashmoushy, H., Zhang, Z., Thomas, C.R., 1998. Micromanipulation measurement of the mechanical properties of baker's yeast cells. Biotechnol. Tech. 12, 925–929. https://doi.org/10.1023/A:1008825830928.

Melendres, A.V., Honda, H., Shiragami, N., Unno, H., 1991. A kinetic analysis of cell disruption by bead mill. Bioseparation 2, 231–236.

Michels, M.H.A., Slegers, P.M., Vermuë, M.H., Wijffels, R.H., 2014. Effect of biomass concentration on the productivity of Tetraselmis suecica in a pilot-scale tubular photobioreactor using natural sunlight. Algal Res. 4, 12–18. https://doi.org/10.1016/j.algal.2013.11.011.

Michels, M.H.A., Van Der Goot, A.J., Norsker, N.H., Wijffels, R.H., 2010. Effects of shear stress on the microalgae Chaetoceros muelleri. Bioprocess Biosyst. Eng. 33, 921–927. https://doi.org/10.1007/s00449-010-0415-9.

Michels, M.H.A., van der Goot, A.J., Vermuë, M.H., Wijffels, R.H., 2016. Cultivation of shear stress sensitive and tolerant microalgal species in a tubular photobioreactor equipped with a centrifugal pump. J. Appl. Phycol. 28, 53–62. https://doi.org/10.1007/s10811-015-0559-8.

Middelberg, A.P.J., 1995. Process-scale disruption of microorganisms. Biotechnol. Adv. 13, 491–551. https://doi.org/10.1016/0734-9750(95)02007-P.

Montalescot, V., Rinaldi, T., Touchard, R., Jubeau, S., Frappart, M., Jaouen, P., Bourseau, P., 2015. Optimization of bead milling parameters for the cell disruption of microalgae: process modeling and application to Porphyridium cruentum and Nannochloropsis oculata. Bioresour. Technol. 196, 339–346. https://doi.org/10.1016/j.biortech.2015.07.075.

Pan, Z., Huang, Y., Wang, Y., Wu, Z., 2017. Disintegration of Nannochloropsis sp. cells in an improved turbine bead mill. Bioresour. Technol. 245, 641–648. https://doi.org/10.1016/j.biortech.2017.08.146.

Phong, W.N., Show, P.L., Ling, T.C., Juan, J.C., Ng, E.P., Chang, J.S., 2018. Mild cell disruption methods for bio-functional proteins recovery from microalgae—recent developments and future perspectives. Algal Res. 31, 506–516. https://doi.org/10.1016/j.algal.2017.04.005.

Postma, P.R., Miron, T.L., Olivieri, G., Barbosa, M.J., Wijffels, R.H., Eppink, M.H.M., 2015. Mild disintegration of the green microalgae Chlorella vulgaris using bead milling. Bioresour. Technol. 184, 297–304. https://doi.org/10.1016/j.biortech.2014.09.033.

Postma, P.R., Suarez Garcia, E., Safi, C., Yonathan, K., Olivieri, G., Barbosa, M.J., Wijffels, R.H., Eppink, M.H.M., 2017. Energy efficient bead milling of microalgae: effect of bead size on disintegration and release of proteins and carbohydrates. Bioresour. Technol. 224, 670–679. https://doi.org/10.1016/j.biortech.2016.11.071.

Schneider, N., Fortin, T.J., Span, R., Gerber, M., 2016. Thermophysical properties of the marine microalgae Nannochloropsis salina. Fuel Process. Technol. 152, 390–398. https://doi.org/10.1016/j.fuproc.2016.06.039.

Shiu, C., Zhang, Z., Thomas, C.R., 2002. Bacterial Species. In: Durieux, Alain, Simon, Jean P. (Eds.), Applied Microbiology. Kluver Academic Pu, pp. 155–162.

Smith, A.E., Zhang, Z., Thomas, C.R., Moxham, K.E., Middelberg, A.P.J., 2000. The mechanical properties of Saccharomyces cerevisiae. Proc. Natl. Acad. Sci. 97, 9871–9874. https://doi.org/10.1073/pnas.97.18.9871.

Suarez Garcia, E., Leeuwen, J.v., Safi, C., Sijtsma, L., Eppink, M.H.M., Wijffels, R.H., van den Berg, C., 2018. Selective and energy efficient extraction of functional proteins from microalgae for food applications. Bioresour. Technol. 268, 197–203. https://doi.org/10.1016/j.biortech.2018.07.131.

Vanthoor-Koopmans, M., Wijffels, R.H., Barbosa, M.J., Eppink, M.H.M., 2013. Biorefinery of microalgae for food and fuel. Bioresour. Technol. https://doi.org/10.1016/j.biortech.2012.10.135.

Wang, C., Lan, C.Q., 2018. Effects of shear stress on microalgae – a review. Biotechnol. Adv. 36, 986–1002. https://doi.org/10.1016/j.biotechadv.2018.03.001.

Yamamoto, Y., Soda, R., Kano, J., Saito, F., 2012. DEM simulation of bead motion during wet bead milling using an enlarged particle model. Int. J. Miner. Process. 114–117, 93–99. https://doi.org/10.1016/j.minpro.2012.10.001.

Zinkoné, T.R., Gifuni, I., Lavenant, L., Pruvost, J., Marchal, L., 2018. Bead milling disruption kinetics of microalgae: process modeling, optimization and application to biomolecules recovery from Chlorella sorokiniana. Bioresour. Technol. 267, 458–465. https://doi.org/10.1016/j.biortech.2018.07.080.